ANALYSIS OF THE FLOW IN LIQUID PROPELLANT ENGINE SWIRL INJECTORS USING CFD

John Elmer Ccasa Infantes
National Institute for Space Research – INPE
Caixa postal 515, CEP 12201-970 São José dos Campos – SP Brazil
johnc@dem.inpe.br

José Nivaldo Hinckel
National Institute for Space Research – INPE
Caixa postal 515, CEP 12201-970 São José dos Campos – SP Brazil
hinckel@dem.inpe.br

Abstract. *The design of injector elements plays a crucial role in the design of liquid propellant engines. The consequences of a poor injector design may range from losses of engine performance to engine failure. Swirl injectors were chosen in this project due to the good atomization and mixing characteristics of this type of injectors. Sizing and design procedures based on analytical formulas derived from non-viscous (Euler) conditions are widely used. For mass flows above 10 g/s, this model shows good agreement with the experimentally obtained mass flows. For lower mass flows the viscous effects become progressively more relevant, resulting in large difference between calculated and measured mass flow. In this work we compare the results of mass flow obtained from ideal analytical model, with those obtained by computational fluid dynamics analyses – CFD and experimental data. All calculations were carried out for a 200 newton bipropelente rocket engine. The software of CFD CFX-5.7, based on the theory of finite volumes, is used to analyze behavior of the flow inside the injetors. A cavitação model is implemented and the viscous effects are considered.*

Keywords: *swirl injector, rocket engine, liquid propellant, CFD, finite volumes.*

1. Introduction

The main challenge for the design and production of bipropellant rocket engines for systems of attitude and orbit control of satellites, is obtaining a reliable mechanism for thermal protection of the wall of the combustion chamber with minimum loss of energetic performance of the engine. Due to the low mass flow of the propellants and to the large exposed area of the thrust chamber, the mechanism of regenerative cooling cannot be used in this type of engine. On the other hand, the temperature of the combustion products can reach up to 3000^{o} C; much higher than the working temperature of the structural materials used in the production of combustion chambers. The temperature attained by the wall of the chamber results from the accommodation of this to the conditions of thermal loads imposed by convection and radiation of the combustion products inside the chamber and conduction convection and radiation to the environment.

Mechanisms that limit the temperature of the combustion chamber to values compatible with the working temperature of the materials used in the production of the combustion chamber must be employed for the operation of these engines for long periods of time

The main mechanism used for the reduction of the thermal load on the combustion chamber wall is the reduction of the mixture ratio through the injection system, with the consequent reduction of temperature of the combustion products. This lower mixture ratio, (O/F), is accompanied by a decrease of the energetic performance of the propellants since part of the available energy in the propellants is not released, due to incomplete combustion.

An alternative to reduce the loss of energetic performance is the use of a radial stratification of the mixture ratio so that the mass flow of the central region, that doesn't enter in contact with the wall, burns with mixture ratio close to the stoichiometric ratio. The fluid layer that flows close to the wall burns with a lower mixture ratio and consequently with a lower temperature.

The practical realization of this mechanism however is difficult to achieve because of the discrete nature of the injection process. Since the distribution of the injector elements in the injector plates is not continuous, a loss of symmetry occurs. This loss of symmetry increases the mixing process between the hot gas flow in the central part of the chamber and the cooler layer near the wall. Because of this lack of symmetry, oxidizer rich streams may break the fuel rich layer near the wall creating local hot spots.

In centrifugal injectors the propellants are introduced in the combustion chamber in the form of a thin film with conical geometry instead of discrete jets as in jet injectors. The organization of the element injectors in the injection face determines the quality of the mixture and the resulting radial flow stratification.

Computational fluid dynamics software packages - CFD have gained considerable acceptance in the analyses in different research areas: space, automotive, biomedical, atmosphere etc. The complex geometry of the distribution channels in the injector plate renders the models for the fluid flow intractable for analytical solution. With the utilization of the software of CFD *CFX-5.7®* the flow inside the injector elements is solved with less restrictive boundary conditions and simplifying hypotheses regarding viscous dissipation. To treat the large pressure variation inside the vortex chamber, a cavitation model was implemented. Viscous effects not taken into account in the analytical model are included in the numerical solution of the flow.

The steady state solution for the flow inside the injector element is presented and discussed. The viscous dissipation effects and losses of total pressure inside the injector element are illustrated.

2. Injector plates of liquid propellants rocket engine

The injector head of a liquid propellant engine is responsible for promoting the atomization and mixing of the propellants. The efficiency of the injector head is directly related to the complete burn of the propellants in the combustion chamber. Factors as: mixture ratio, homogeneity of the distribution of the mass flow, the quality of atomization of the propellants, are characteristic that influence this efficiency.

Two types of injectors are used commonly: Jet injectors, in several impinging configurations are used mainly in American and European engine; swirl injectors are used predominantly in Russian rockets engine. For the jet injector type, there is a vast literature, where its main characteristics of performance are examined. For the swirl injector there is scarce literature available and most of it from Russian sources, a large part of which is in the Russian language. Due to the good atomization and mixing characteristics of the propellants, in the present work the solution of centrifugal injector elements was adopted. The publications of Bazarov, 1997; Bazarov and Yang, 1998; Bazarov and Hinckel, 2001, treat of these injectors.

Due to the small value of diameter of the chamber, the production of the injector elements and welding of the plates containing the labyrinth of distribution of the propellants present great difficulty of execution. To make possible the placement of a large number of injector elements with different mixture ratios, the vortex chamber, entrance channels and exit nozzle of the swirl injector element are machined directly on the face of the injector plates. The plates are subsequently joined by vacuum diffusion welding.

2.1. Description of the injector plates of a 200 newton rocket engine

The injector head consists of an oxidizer plate, a fuel plate and a distribution plate. The oxidizer and fuel plates have a central injector and six peripheral injectors distributed in a concentric ring. The oxidizer and fuel elements form pair with a common axis. The nozzle of the oxidizer element is located inside the empty nucleus of the fuel element. Additionally the fuel plate has a curtain of fuel injected close to wall of the combustion chamber as shown in the Fig. 1, plate of oxidizer and fuel respectively. The central injector has a mixture ratio of 2.5:1 and a mass flow of approximate of 35 g/s; approximately 50% of the total propellant mass. The peripheral injector elements have a mixture ratio of 2:3. The injection of the fuel curtain is made through three vortex chamber and injected in the combustion chamber by breaches close to the wall. The breaches are sized for an injection velocity less than 1 m/s and with small angle with respect to the axis of the combustion chamber (Hinckel *et al.* 2002). The distributions plate contains the propellant entrance ports and directs the propellant flow to the fuel and oxidizer plates.

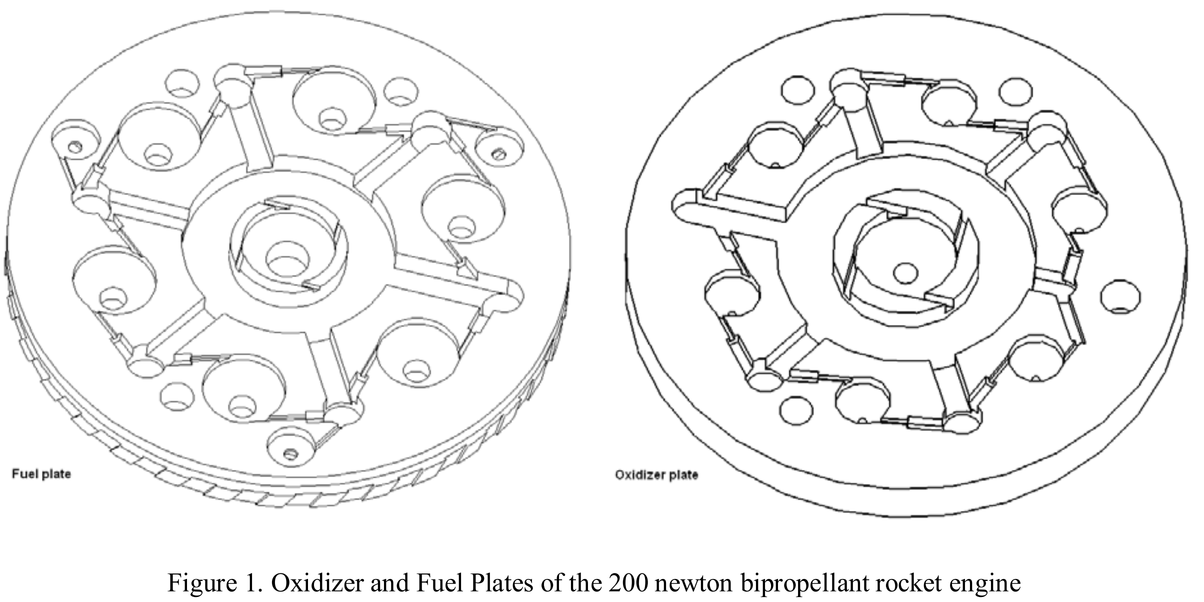

Figure 1. Oxidizer and Fuel Plates of the 200 newton bipropellant rocket engine

2.2. Finite volumes method – Conservation equations

The analytical solution for the flow inside the nozzle is based on several simplifying hypothesis; no viscosity, radial symmetry, homogeneous radial and axial velocities. Numerical computational methods allow the inclusion of viscous effects and the exclusion of the restrictive hypotheses of radial symmetry and uniform radial and axial velocities. The steady state solution of the flow inside the injector element is obtained using the software package *CFX-5.7*. In this paper we present and discuss the results for the central injector elements. The use of a cavitation model is very important in the solution to this problem since it permits the solution to the free surface of the liquid flow inside the vortex chamber and nozzle. The volume fraction variable of the solution represents the vapor fraction in each computational cell. It has a value of 1 for the liquid region and drops to zero in low pressure, vapor region.

In the finite volumes method the approximate equations are obtained through the integration of the equations of conservation of the involved properties (mass, momentum, energy, etc) in an elementary control volume.

The local equations of mass, momentum and energy conservation can be written as follows in a stationary frame (manual *CFX-5.7* and Schlichting, 1979):

Equation of conservation of mass:

$$\frac{\partial \rho}{\partial t} + \nabla \cdot (\rho \mathbf{u}) = 0 \tag{1}$$

Conservation of momentum:

$$\frac{\partial}{\partial t}(\rho \mathbf{u}) + \nabla \cdot (\rho \mathbf{u} * \mathbf{u}) = \nabla \cdot (-p\boldsymbol{\delta} + \mu(\nabla \mathbf{u} + (\nabla \mathbf{u})^{\tau})) + \mathbf{s}_M \tag{2}$$

Conservation of energy:

$$\frac{\partial}{\partial t}(\rho h_{tot}) - \frac{\partial p}{\partial t} + \nabla \cdot (\rho \mathbf{u} h_{tot}) = \nabla \cdot (\lambda \nabla T) + (\nabla \cdot (\mu(\nabla \mathbf{u} + (\nabla \mathbf{u})^{\tau} - \frac{2}{3}\nabla \cdot \mathbf{u}\boldsymbol{\delta})\mathbf{u}) + \mathbf{s}_E) \tag{3}$$

In the equations above ρ is the density, t is time, $\mathbf{u}$ is a vector of total velocity, p is pressure, λ is thermal conductivity, T is the temperature, μ is the dynamic viscosity coefficient, $\boldsymbol{\delta}$ is the identity matrix, τ indicates transposed, $\mathbf{S}_M$ e $\mathbf{S}_E$ represent moment and energy sources and h_{tot} is defined as the specific total enthalpy, which for the general case of variable properties and compressible flow is given in terms of the specific static enthalpy (thermodynamic), h, expressed by:

$$h_{tot} = h + \frac{1}{2}\mathbf{u}^2 = 0 \tag{4}$$

where:

$$h = h(p, T) \tag{5}$$

2.3. Description of the finite volume models and boundary conditions

The solution was obtained for separate element injector for the fuel and oxidizer plates. For the oxidizer plate the global solution for the flow in all injector elements and distribution labyrinth was also obtained. The global solution was obtained to evaluate the losses of total pressure in the distribution labyrinth and the effect of these pressure losses in the total mass flow of each peripheral injector. In all the simulations, water was used as working fluid.

The boundary condition used in the CFD model is the total pressure at the entrance and exit of each injector element or distribution channel of the labyrinth. Therefore a boundary condition of total pressure of 0.7 MPa was imposed at the entrance channel of the individual injector and injector plate. The exit boundary condition is the static pressure of 0 MPa. Water vapor and water properties, both the temperature of 25^{o} C are used.

3. Results

Figure 2 shows the distribution of the total pressure in oxidizer plate. As can be observed, the losses of total pressure occur mainly inside the vortex chamber and exit nozzle of the injectors.

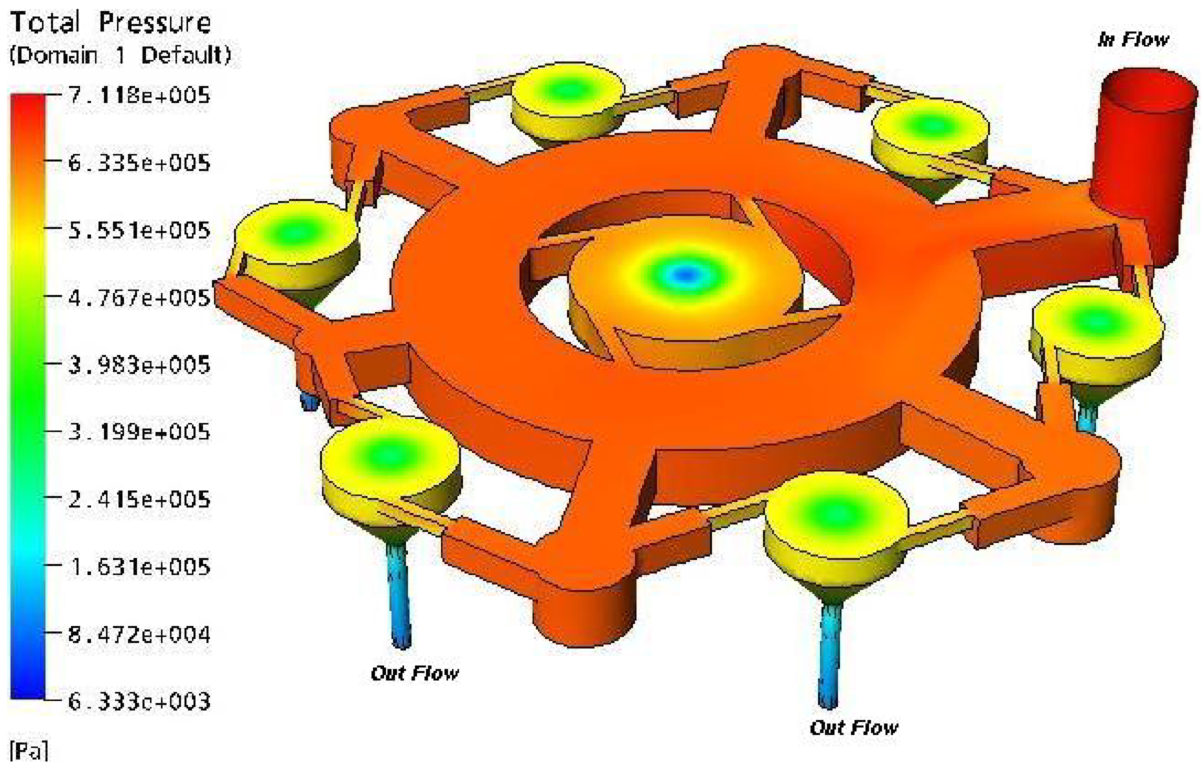

Figure 2. Distribution of the total pressure in the oxidizer plate

Figures 3 and 4 show the distribution of the pressure, velocity and volume fraction in the central injector elements of the oxidizer and fuel plates respectively. The solution was obtained with the pressure boundary condition applied at the entrance channel and nozzle exit of the injector elements. As can be observed the radial component of velocity is very small everywhere inside the injector except near the top wall and the bottom conical section of the swirl chamber. The azimuthal velocity increases from the entrance channel towards the central region of the injector. Unlike the analytical solution, where the azimuthal velocity increases with the inverse or the radial distance, it reaches a maximum value and then decreases due to viscous dissipation. The axial velocity is large only in the exit nozzle. The volume fraction shows the hollow nucleus in the center of the swirl chamber and nozzle. It should be noted that the fuel injector geometry is significantly different from the oxidizer. This is due to the restriction that the envelope of the oxidizer nozzle must fit inside the swirl chamber of fuel injector. From Fig. 4e it is clear that the envelope of the oxidizer nozzle is completely inside de hollow nucleus of the flow in the fuel element. Therefore the disturbance caused by the oxidizer nozzle inside the fuel element swirl chamber is very small.

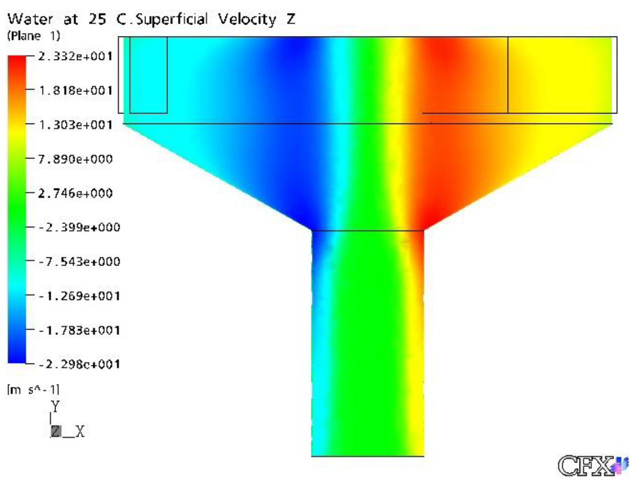

(a) Azimuthal velocity

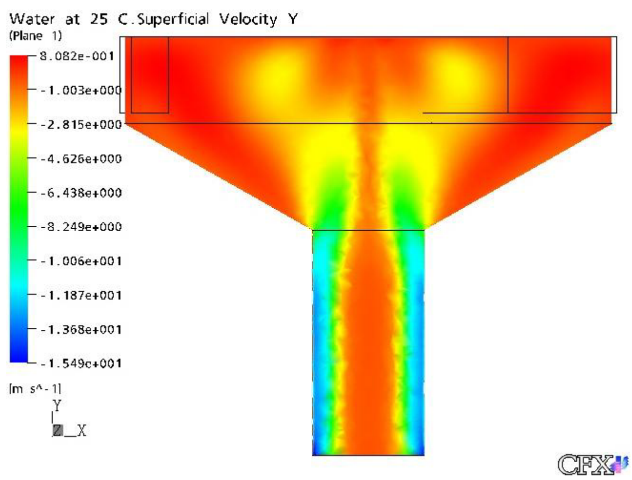

(b) Axial velocity

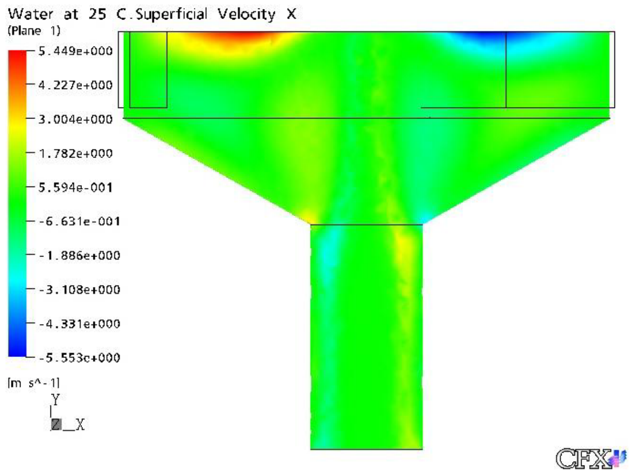

(c) Radial velocity

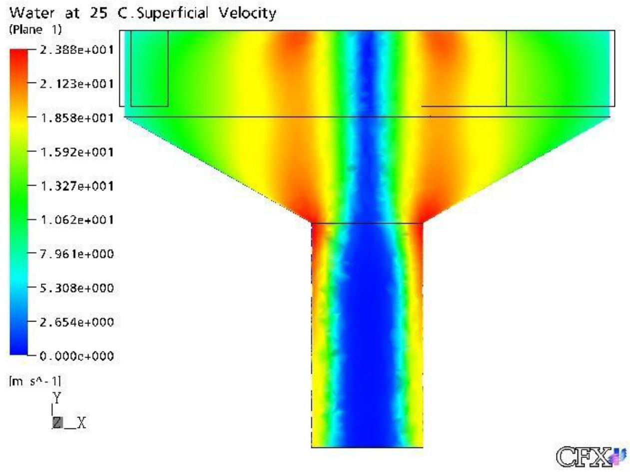

(d) Modulus of total velocity

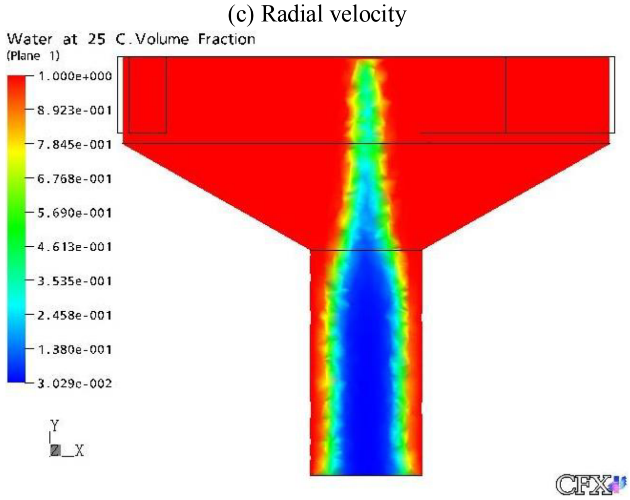

(e) Volume fraction

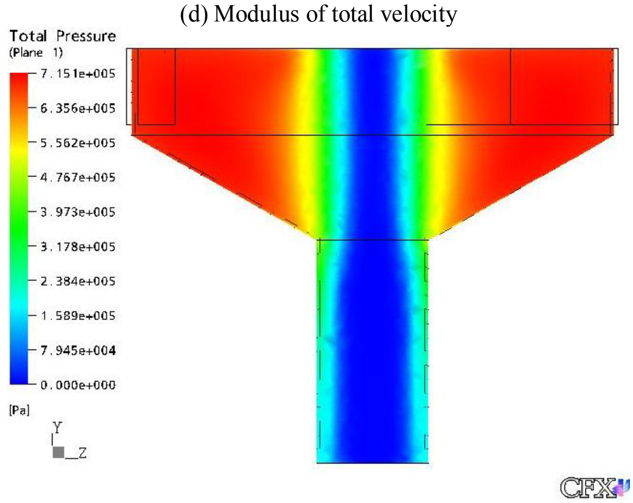

(f) Total pressure

Figure 3. Distribution of the pressure, velocity and volume fraction of the central oxidizer injector – Transversal section

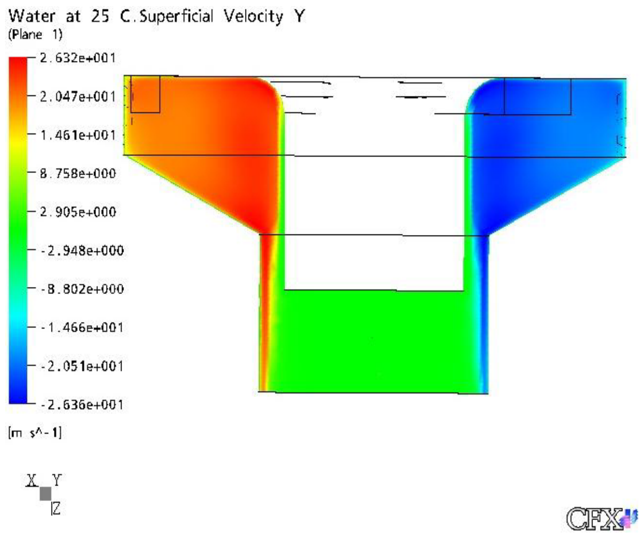

(a) Azimuthal velocity

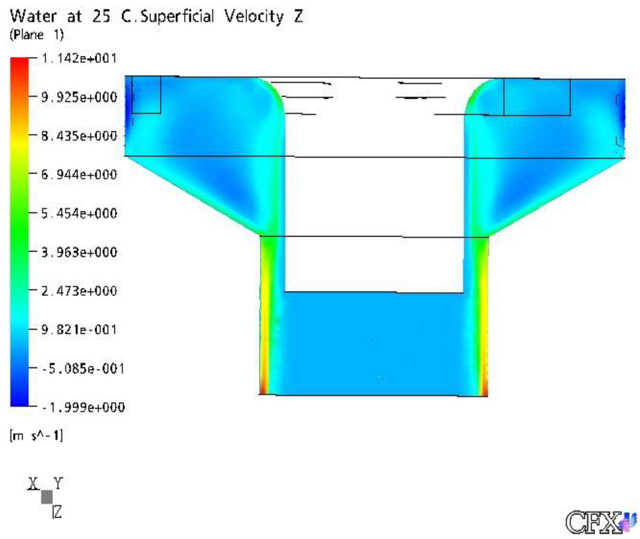

(b) Axial velocity

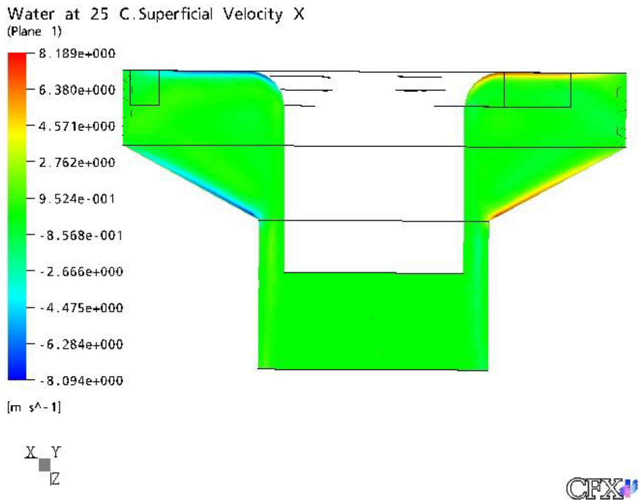

(c) Radial velocity

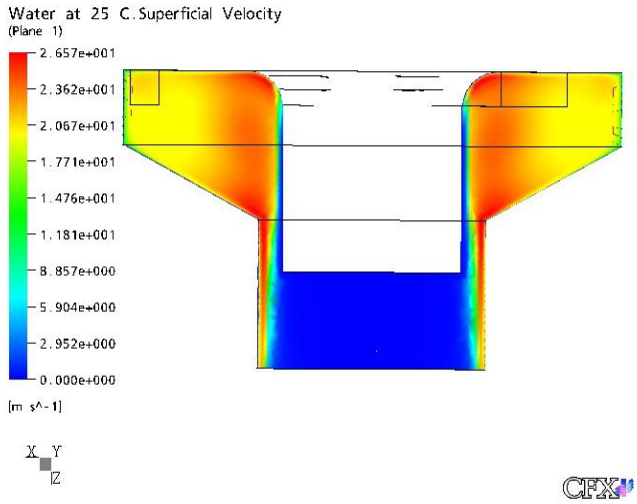

(d) Modulus of total velocity

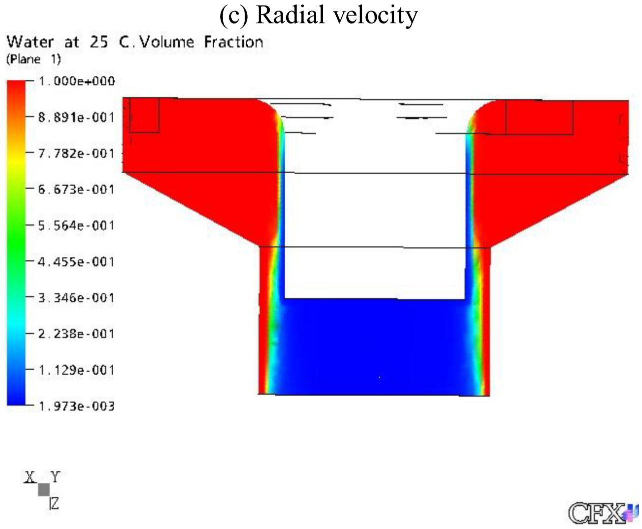

(e) Volume fraction

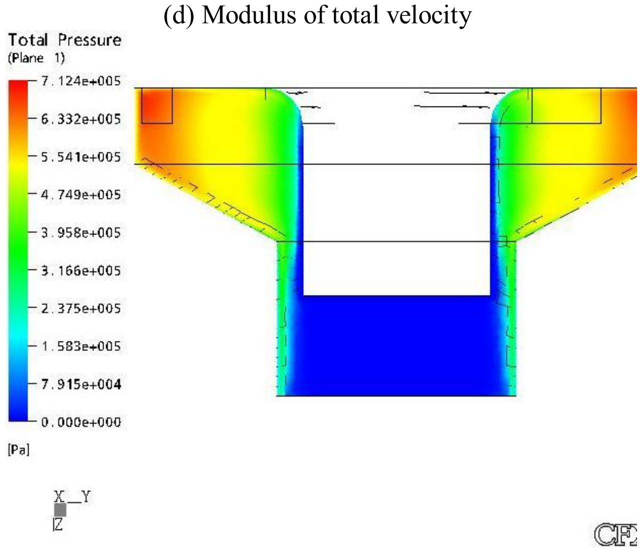

(f) Total pressure

Figure 4. Distribution of the pressure, velocity and volume fraction of the central fuel injector – Transversal section.

Figures 5 and 6 show the profile of the total and static pressure as well as the variations of velocity along the radius in sections 1-1 and 2-2 of the vortex chamber and exit nozzle of the central injector oxidizer element. The variables u v and w are the azimuthal, axial and radial velocity components; z is the radius. As can be observed in Fig. 5a and Fig. 6a, the pressure drops towards the central region of the injector (hollow nucleus in the center of the swirl vortex chamber and nozzle). In Fig. 5b, the resultant velocity is determined mainly by the azimuthal component. The radial and axial velocities are very small in the swirl chamber. The axial component has large value only in the nozzle as shown in Fig. 6b. It is important to indicate that Cartesian coordinates was used in the model, reason for which the component azimuthal and radial they appear with opposite signal in relation to the axis z = 0.

Table 1, shows in detailed form the results of mass flow of the entrance channels and the mass flow in the exit injectors of the oxidizer and fuel plates obtained through *CFX*. The discretisation and the number of iterations for convergence of the model are also shown. Two convergence criteria were used. First, when the variation of velocity from one iteration to the next was less than 1e-5 (the error norm) and second, when the mass flow imbalance between the entrance and the exit of the injector was less than 1%. It can be verified that after the mass imbalance falls bellow 1% the changes of the error norm are not significant.

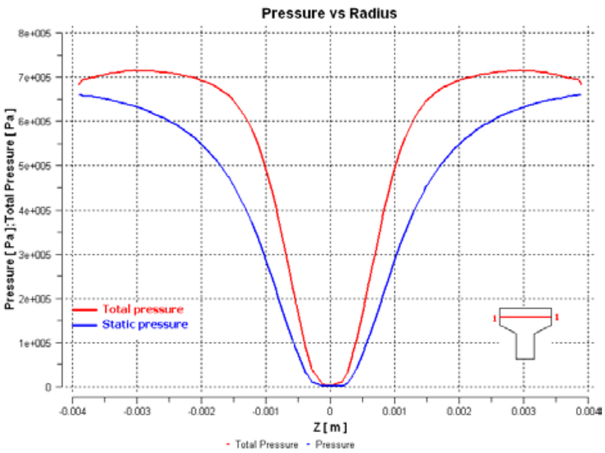

(a) Pressure vs. Radius

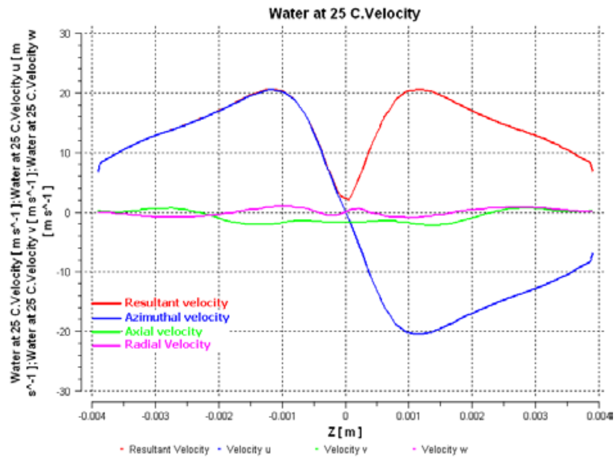

(b) Velocity vs. Radius

Figure 5. Development of the pressure and velocity component in the central injector of oxidizer - Section 1-1

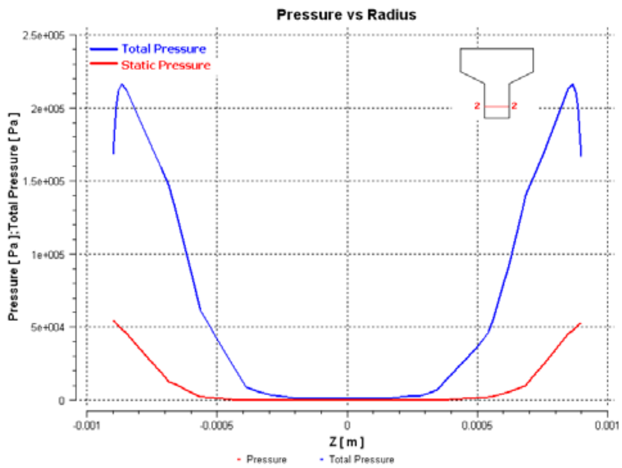

(a) Pressure vs. Radius

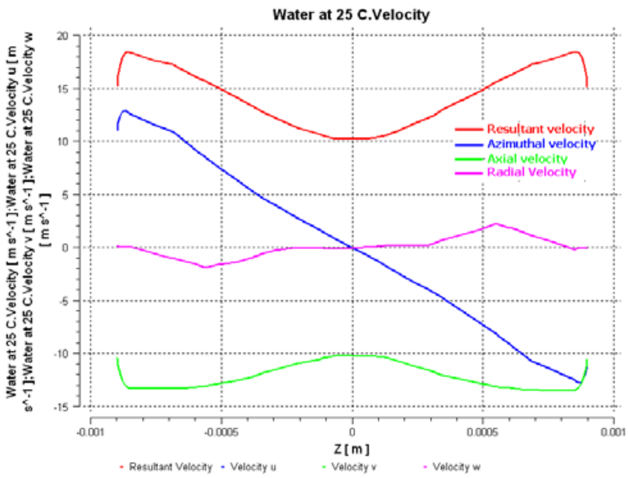

(b) Velocity vs. Radius

Figure 6. Development of the pressure and velocity component in the central injector of oxidizer - Section 2-2.

Table 1. Results the mass flow of the oxidizer injector plate gives by *CFX*.

Plate	Oxidizer plate		Fuel plate	
Injector	Central injector	Peripheral injector	Central injector	Peripheral injector
Element number	179687	66895	201900	66308
Iteration	377	425	397	535
Num. input channel	4	2	4	2
Mass in1 (kg/s)	4.855E-03	2.055E-03	3.293E-03	2.583E-03
Mass in2 (kg/s)	4.869E-03	2.055E-03	3.281E-03	2.574E-03
Mass in3 (kg/s)	4.848E-03	------	3.285E-03	------
Mass in4 (kg/s)	4.826E-03	------	3.453E-03	------
Mass Out (kg/s)	19.60E-3	4.094E-03	12.731E-03	5.127E-03

Tables 2 and 3 show the results of mass flow of the injectors measured in hydraulic tests and the results of the analytic and CFD models of oxidizer and fuel plates respectively.

Table 2. Comparison of the results of outflow of the oxidizer plate.

Plate	Oxidizer plate			Error [%]	
Mass flow injector	Measured	Analytical	CFD	Error 1[(1)]	Error 2[(2)]
Peripheral injector (kg/s)	2.827E-03	1.662E-03	4.094E-03	41.21	-41.82
Central injector (kg/s)	1.888E-02	1.906E-02	1.968E-02	-0.94	-4.23

[(1)]Error measured in relation to the analytical model
[(2)]Error measured in relation to the CFD model

Table 3. Comparison of the results of outflow of the fuel plate.

Plate	Fuel plate			Error [%]	
Mass flow injector	Measured	Analytical	CFD	Error 1[(1)]	Error 2[(2)]
Peripheral injector (kg/s)	4.602E-03	3.207E-03	5.127E-03	30.32	-11.40
Central injector (kg/s)	1.335E-02	1.225E-02	1.273E-02	8.22	4.62

[(1)]Error measured in relation to the analytical model
[(2)]Error measured in relation to the CFD model

4. Comments and Conclusions

The mass flow results obtained through *CFX-5.7* for the central injector of the oxidizer and fuel plate present a good agreement with the measured values. The difference doesn't surpass of 4,62% in relation to the measured model. The peripheral injectors present a larger discrepancy when we compared the experimental model with the analytic model what it demonstrates, as it was expected, that the viscous effects are more important in low mass flow. For mass flow greater than 10 g/s the viscous effects are less significant.

Due to the limit in number of pages the graphical representation of the pressure and velocity for the peripheral injector elements are not shown here.

The results obtained from the computational model are very helpful for understanding and explaining the physical phenomena inside the vortex chamber and nozzle of the injector.

The results obtained show that for large mass flow injectors (more than 5 g/s), good agreement is observed between analytical, numerical and experimental results. For small mass flows, the results obtained from the analytical models are substantially smaller than the measured values. In this case it is also clear that the numerical results are much closer to the experimental results than the analytical results. Due to the large pressure drop in the vortex chamber, the effect of viscosity is to increase the mass flow for the same geometry and pressure drop; the opposite effect that occurs in the jet injector.

It should also be pointed out that for the small mass flow injectors, with dimensions in the order of 200 µm, it is much harder to attain the required precision of machining and other fabrication processes.

In general the discrepancies of the analytical, numerical and experimentally measured values are consequences of hypotheses, simplifications, fabrication errors and inherent errors to the measurement process.

To improve the results more tests and simulations should be made in the experimental and CFD models.

5. References

Bazarov, V.G., 1997, “Hydraulics of swirl propellant injector”, 9th Annual Conference of Propulsion Engineering Research Center of the Pennsylvania State University, Cleveland, OH, USA, October.

Bazarov, V.G. and Hinckel, J.N., 2001, Hydraulics of injectors, Class notes. National Institute for Space Research. São José dos Campos – SP, Brasil.

Bazarov, V.G. and Yang, V., 1998, “liquid Propellant Rocket Engine Injector Dynamics”, Journal of Propulsion and Power, V. 14, pp. 797-806.

CFX-5.7, 2005, Manual of Computer Dynamics Fluid.

Hinckel, J.N., Kozlov, A.A., Moraes, F.J.V. and Cardoso, H.P., 2002, “Development of a 200 Newton liquid Bipropellant Thruster”, 9th Congresso Brasileiro de Engenharia e Ciências Térmicas - ENCIT, Caxambu - MG, Brasil – CD Rom.

Schlichting, H., 1979, “Boundary Layer Theory”, Ed. McGraw-Hill Book Company, 817 p.

6. Responsibility notice

The authors are the only responsible for the printed material included in this paper.